Biomedicine & Pharmacotherapy 89 (2017) 162–176

Available online at
ScienceDirect
www.sciencedirect.com

Elsevier Masson France
EM|consulte
www.em-consulte.com/en

A novel approach towards design, synthesis and evaluation of some Schiff base analogues of 2-aminopyridine and 2-aminobezothiazole against hepatocellular carcinoma

Shinu Chacko*, Subir Samanta

Division of Pharmaceutical Chemistry, Department of Pharmaceutical Sciences and Technology, Birla Institute of Technology, Mesra, Ranchi, Jharkhand 835215, India

ARTICLE INFO

Article history:
Received 1 December 2016
Received in revised form 8 January 2017
Accepted 17 January 2017

Keywords:
Hepatocellular carcinoma
Schiff's base
Anti-oxidant
DPPH diethylnitrosamine
Aspartate transferase
Alanine transferase
Reactive oxygen species
Histopathology

ABSTRACT

Hepatocellular carcinoma is the most common primary malignancy of the liver with poor prognosis. In this study novel, Schiff's bases of 2-aminopyridine (SSSC-26 to 31) and 2-aminobenzothiazole (SSSC-32 to 37) were designed, synthesised and evaluated for antioxidant potential using DPPH method, and anti-hepatocellular carcinoma property using diethylnitrosamine (DEN) induced hepatocellular carcinoma rat model. The in-silico pharmacokinetic, rule of five and toxicity studies reveals that all the leads have an excellent intrinsic quality and sufficient structural features necessary for an oral activity. Molecular docking studies of all compounds into the ligand binding pocket of checkpoint kinase1 and vascular endothelial growth factor receptor-2 was also performed using Schrodinger software suite *v*8.5, and which have shown good Glide scores. Further compounds were synthesised based on the docking score and ADMET profile. The 1,1-diphenyl2-picrylhydrazil (DPPH) scavenging study was carried out, and results showed that SSSC-29 (IC_{50}-63.60) and SSSC-33 (IC_{50}-60.32) were having good anti-oxidant potential in comparison with ascorbic acid (IC_{50}-55.27). SSSC-33 further evaluated for anti-cancer potential against diethylnitrosamine (200 mg/kg bw) induced hepatocellular carcinoma in rats. The biochemical, histopathological and morphological data showed that SSSC-33 can reverse the changes occurred in the cancerous liver significantly. All these findings suggested that SSSC-33-((benzo[d]thiazol-2-ylimino) methyl)phenol) could be a potential compound in combating the oxidative damage of hepatic cells occurred due to the development of hepatocellular carcinoma induced by a chemical carcinogen, DEN.

1. Introduction

Hepatocellular carcinoma (HCC), a primary malignancy of the liver, is the fifth most common cancer in men and seventh in women. Poor prognosis is the main reason for decreased cure rate of HCC and occurrence of approximately more than 50, 000 new cases of HCC worldwide every year [1]. Globally, death rate from all other common cancers (such as lung, breast, and prostate cancers) is declining, whereas mortality rate from liver cancer are increased by 2.8 and 3.4 percentage per year respectively in men and women [2]. Most cases of HCC develop in the liver having chronic damage with alcoholic liver disease, non-alcoholic fatty liver, hepatitis B (accounts for most 50% of all cases of HCC worldwide) and hepatitis C infection [3]. Multiple treatment options are available for HCC like surgical resection, locoregional ablation, cytotoxic chemotherapy (e.g., sorafenib) and liver transplantation but the later diagnosis of HCC is the major limitation for the success. At an advanced stage, sorafenib, a multi-kinase inhibitor, is the only US FDA-approved therapy [4]. In the study conducted by Xiao-Ke Guo et al., natural molecule like Gambogic acid (GA) and its derivatives have been proved as apoptotic agent against HepG2 cell lines [5].

Reactive oxygen species (ROS) includes superoxide anion radical ($O_2^{-\bullet}$), singlet oxygen (O), hydrogen peroxide (H_2O), and the highly reactive hydroxyl radical ($^{\cdot}OH$) play a significant role in carcinogenesis [6]. Oxidative stress occurs due to excess ROS production, depletion of antioxidants (like superoxide dismutase) or both and subsequent imbalance in the average level of ROS and antioxidants. Especially in HCC amount of ROS is more due to permanent damage of liver, a major metabolising organ. Compounds of having antioxidant property may have anti-HCC activity due to its free radical scavenging activity [7].

* Corresponding author.
E-mail address: shinu10015@bitmesra.ac.in (S. Chacko).

http://dx.doi.org/10.1016/j.biopha.2017.01.108
0753-3322/

Schiff bases or Azomethines, first reported by Hugo Schiff in 1864, broadly display range of biological activities such as anticancer, antifungal, antibacterial, antimalarial, antiviral, anti-pyretic, anti-inflammatory characteristics [8]. Schiff's bases with general formula RHC=N—R' (Imine group) are the class of compounds formed by the condensation between the primary amine and carbonyl compounds [9]. The lone pair of electrons present in sp^2 hybridised orbital of the nitrogen atom in the imine group responsible for its chemical and biological properties [10]. The chelating property of Schiff bases plays a significant role in its antioxidant activity, and this will be helpful in the development of compounds with anti-hepatocellular carcinoma.

In this work, some novel Schiff's bases based on 2-amino-pyridine and 2-aminobenzothiazole with various aldehydes are designed and evaluated theirs *in silico* toxicity and absorption, distribution, metabolism and excretion (ADME) properties using Protox and QikProp software respectively. Further, we docked the hits with checkpoint 1 (Chek1) and vascular endothelial growth factor receptor (VEGFR) using Schrodinger software suite *v*8.5 [11]. The leads having good docking score and reasonable ADMET property was selected for synthesis. The compounds were characterised by ^{1}H NMR, ^{13}C NMR, Mass spectral and elemental analysis. Compounds were then screened for its anti-oxidant property by 1,1-diphenyl-2-picrylhydrazil (DPPH) [12,13] method using ascorbic acid as standard. Subsequently evaluation of anti-HCC activity of the best compound by its anti-oxidant property and docking score was performed in DEN-induced HCC rat model [1].

Diethylnitrosamine (DEN) is a chemical carcinogen and DEN-induced HCC in the rat is considered an as well accepted model for the development of drugs against hepatocarcinogenesis. DEN was first hydroxylated to alpha-hydroxy nitrosamine in the presence of cytochrome P450- dependent enzymatic system and which is capable of alkylating DNA structure (Fig. 1). ROS are also generated during this enzymatic process and causes lipid peroxidation and adds up to the hepatocarcinogenesis [1]. DEN-induced HCC rat model to mimic the injury-fibrosis-malignancy cycle. Here, DEN was given to the rat in the period of hepatic cell proliferation, initiated by partial hepatectomy (PH) [14], which followed a necrotizing dose of carbon tetrachloride (CCl_4; hepatotoxin) [15,16]. Trichloromethyl radicals formed by the metabolism of CCl_4 by CYP 450 causes lipid peroxidation and membrane damage [17]. Phenobarbitone sodium (PB) (which increases the expression of CYP 450 enzyme and leads to the enhanced effect of DEN and CCl_4) was also given during induction period for the successful hepatocarcinogenesis.

2. Material and methods

2.1. General information

Docking calculation was carried out on HP Intel® Core 2 due ® processor E3-1200v2 family with 16GB RAMS, 1TB Hard disk, NVIDIA Quadro 2000, Linux. Chem Office (level: Ultra, version: 3.5) was used for drawing and energy minimization of structures. QikProp module of Schrödinger was employed for Absorption, Distribution, Metabolism and Excretion (ADME) prediction and docking studies. ProTox, a web server was the toxicity determining tool used for Lethal Dose, 50% (LD50) calculation in the rat.

All the chemical used for the synthesis and *in vivo* study (DEN, CCl_4, and phenobarbitone sod.) were of analytical grade purchased from Sigma-Aldrich. The progress of the reaction was determined by thin layer chromatography (TLC) on silica gel plates in various solvents. UV-lamp (λ = 254–365 nm) was used for visualisation of TLC plate and iodine vapour or ninhydrin reagent as detecting agent. Melting points were determined on OptiMelt (Stanford Research Systems, California) and were uncorrected. ^{1}H NMR (400 MHz) was performed on Bruker Advance 300 instrument (Bruker Instruments Inc., USA) using DMSO-d_6 as solvent and tetramethylsilane (TMS) as an internal standard. Chemical shifts were expressed in parts per million (ppm). Mass spectra were recorded by WATERS-Q-T of Premier-HAB213 using the ESIMS Electrospray Ionization technique.

2.2. Molecular design

2.2.1. ADME prediction

The prediction of ADME (Absorption, Distribution, Metabolism and Excretion) properties are considered to be crucial in the development of a new drug since lots of drugs are being withdrawn from the market due to the inappropriate ADME properties. The

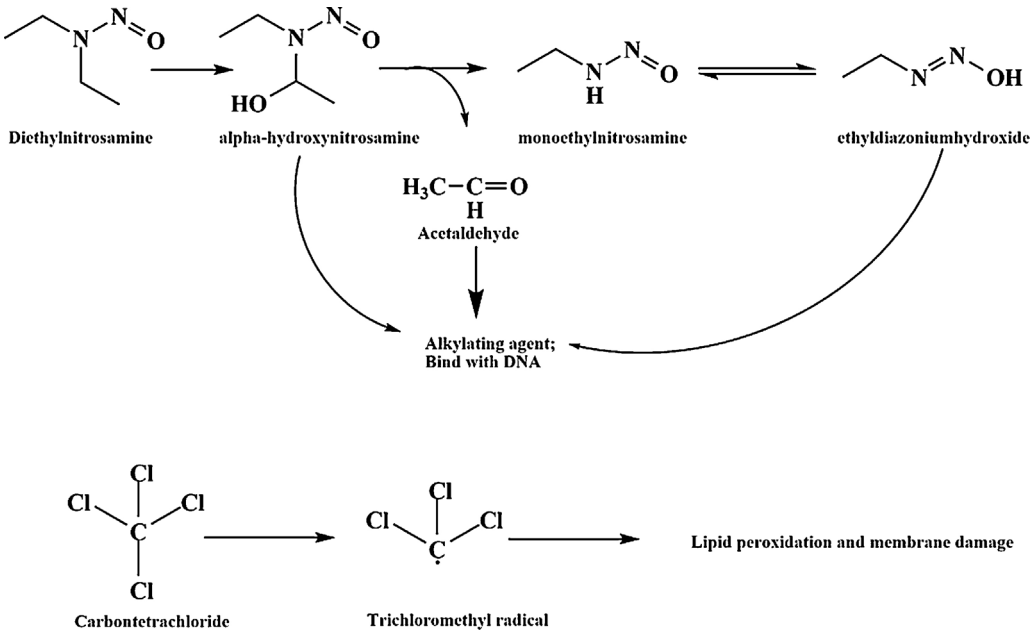

Fig. 1. Metabolism of DEN and CCl_4 in the presence of CYP 450 enzymatic system.

Table 1
Schiff's bases of 2-aminopyridine.

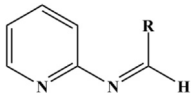

Compound	R	Molecular Formula	Mol. Wt.
SSSC-26	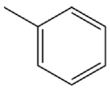	$C_{12}H_{10}N_2$	182.22
SSSC-27	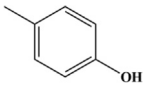	$C_{12}H_{10}N_2O$	198.22
SSSC-28	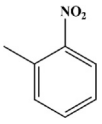	$C_{12}H_9N_3O_2$	227.22
SSSC-29	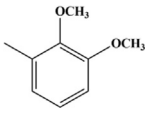	$C_{14}H_{14}N_2O_2$	242.27
SSSC-30	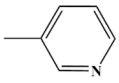	$C_{11}H_9N_3$	183.21
SSSC-31	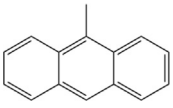	$C_{20}H_{14}N_2$	282.34

ADME properties of the proposed molecules were generated by the QikProp, version 3.0, Schrödinger, LLC, New York, 2005 [18].

2.2.2. Acute rat toxicity prediction

A safer drug should have a high therapeutic index [ratio between dose producing a therapeutic effect (effective dose, 50%, ED_{50}) and dose producing toxic effects (LD_{50}). *In silico* prediction of the LD_{50} in mg/kg in rodents after oral administration was done by ProTox, a web server, for the prediction of oral toxicities of small molecules. Additionally, it provides information about toxicity class using similarity and fragment-based methods and possible toxicity targets. It also suggests the mechanisms involved in toxicity development [19].

2.2.3. Docking studies of the designed molecules

2.2.3.1. Target identification. The crystal structure of the target Proteins, Chk 1 (PDB entry: 1ZYS) [20] and VEGFR-2 (PDB entry: 2QU5) [21], were retrieved from Research Collaboratory for Structural Bioinformatics (RCSB) PDB, a crystallographic database for the three-dimensional (3D) structural data of the primary biological molecules like proteins and nucleic acids (http://www.rcsb.org/pdb/home/home.do).

2.2.3.2. Protein preparation. The crystal structure of the target protein downloaded from PDB was prepared by using the prep wizard of Schrödinger, since it is not suitable for immediate use in molecular modelling calculations. This protein preparation was done by adding missing atoms, removing unwanted chains, water molecules and heterocyclic atoms and set for receptor grid generation. The procedure was completed with an energy minimised protein-ligand complex, to which hydrogen was added subjected to protonation states for ionizable residues, modification of tautomeric forms and the repositioning of the re-orientable hydrogen.

2.2.3.3. Receptor grid generation. Blind docking is performed if information and location about the binding site are unknown. Here, a ligand with known binding modes and active site residues are available with the downloaded crystal structure of protein. It is utilised to create a specified area of the active site (grid) so that search space can be reduced to focus on the region of interest. The processed protein was used for receptor grid generation using Glide 5.0 component of the Schrödinger. The grid defines the binding site of the receptor protein to which ligand has to bind.

2.2.3.4. Ligand preparation. The proposed Schiff's bases (Tables 1 and 2) were drawn in 2D and converted into 3D using Chem Office

Table 2
Schiff's bases of 2-Aminobenzothiazole.

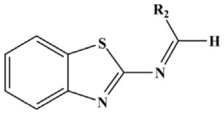

Compound	R_2	Molecular Formula	Mol. Wt.
SSSC-32	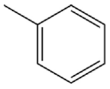	$C_{14}H_{10}N_2S$	238.31
SSSC-33	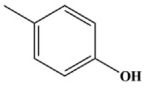	$C_{14}H_{10}N_2OS$	254.05
SSSC-34	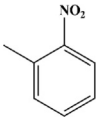	$C_{14}H_9N_3O_2S$	283.31
SSSC-35	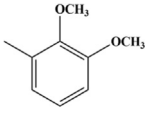	$C_{16}H_{14}N_2O_2S$	298.36
SSSC-36	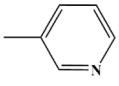	$C_{13}H_9N_3S$	239.05
SSSC-37	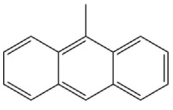	$C_{22}H_{14}N_2S$	338.09

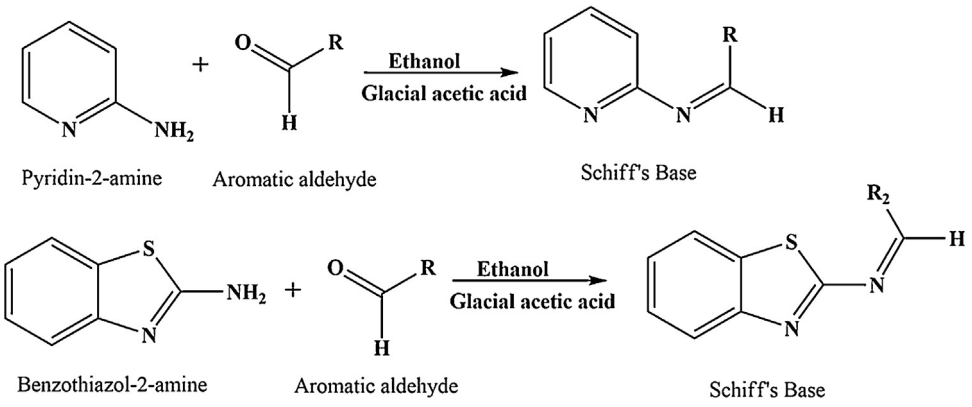

Scheme 1. Synthesis of Schiff's Bases using 2-aminopyridine and 2-aminobenzo thiazole.

10.0. Preliminary energy minimization and molecular dynamics study were done to identify low energy conformers which were saved in mole format using the same software. These molecules were imported into Schrödinger project table, and ligand preparation was carried out using LigPrep 2.2. Fully customised ligand libraries generated were further optimised for computational analysis by including energy minimised tautomeric, stereochemical and ionisation variations.

2.2.3.5. Validation of docking protocol. Docking method was validated by removing the inhibitor bound to the protein from the active site and re-docked it [24] into the *apo*-form of the Chek 1 receptor and VEGFR-2 [25]. The conformation and orientations of the ligand in the docked form were compared to that of the original X-ray crystallographic structure downloaded from PDB.

2.2.3.6. Molecular docking. The generated structures of various conformations of designed molecule were docked into the predicted binding site of the targeted receptor proteins (1ZYS and 2QU5) using Glide, Version 5.0, Schrödinger, LLC, New York, NY, 2008. Docking was done in standard precision (SP) mode. Potential hits were found out based on Glide score [26,27].

2.3. Synthesis of Schiff's bases

2.3.1. General procedure

Various Schiff bases of 2-aminopyridine (SSSC-26 to 31) and 2 −amino benzothiazole (SSSC-32 to 37) were prepared as per the Scheme 1.

A mixture of equimolar quantities of aryl aldehydes (0.01 mol) and 2-aminopyridine/2-Aminobenzothiazole (0.01 mol) in ethanol/methanol (20 mL) was refluxed on a water bath for 6–10 h in the presence of a few drops of glacial acetic acid as catalyst. Thin layer chromatography (TLC) monitored the progress of reaction at an appropriate time interval. After completion of the reaction, the solution was cooled, separated solid was filtered and washed with ice-cold water and dried. Finally, the product thus obtained was recrystallized from ethyl acetate and ethanol in different proportions depending on the nature of the compound [28].

2.3.2. N-benzylidenepyridin-2-amine (SSSC-26)

SSSC-26 was prepared by the condensation of 2-aminopyridine with benzaldehyde in methanol using glacial acetic acid as catalyst. Yield 78%, mp 120 °C, ESI–MS (*m*/*z*): 183.0 [M + H]; ^{1}H NMR (400 MHz, DMSO— d_6): δ (ppm) 10.89 (s, 1H, Ar-N**H**), 7.2-8.3 (m, 4H, Ar-**H**-), 4.3 (s, 2H, N**H**$_2$), 2.7 (s, 1H, −C = S-N**H**-); ^{13}CNMR (125 MHz, DMSO-*d*6): δ (ppm) 165.040 (**C**2-pyridine), 152.580 (**C**-Azomethine), 140.210 (**C**6-pyridine), 131.066 (**C**4-pyridine), 121.793-128.949 (**C**-phenyl), 121.490 (**C**-5 pyridine), 118.985 (**C**-3 pyridine).

2.3.3. 4-((pyridin-2-ylimino)methyl)phenol (SSSC-27)

SSSC-27 was prepared by the condensation of 2-aminopyridine with *p*-hydroxy benzaldehyde in methanol using glacial acetic acid as catalyst. Yield 80%, mp 117 °C, ESI–MS (*m*/*z*): 198.0 [M +]; ^{1}H NMR (400 MHz, DMSO— d_6): δ (ppm) 9.19 (s, 1H, N=C**H**), 8.50 (d, 1H, N—C**H**), 7.73 (t, 1H, C—C**H**), 7.71 (s, 1H,O**H**), 7.3 (t, 1H, N—C—C**H**), 7.40 (d, 1H, C=C**H**) 6.8-7.5 (m, 4H, Ar-**H**-).

2.3.4. N-(2-nitrobenzylidene)pyridin-2-amine (SSSC-28)

SSSC-28 was prepared by the condensation of 2-aminopyridine with 2-nitrobenzaldehyde in methanol using glacial acetic acid as catalyst. Yield 82%, mp 128 °C, ESI–MS (*m*/*z*): 228 [M + H]; ^{1}H NMR (400 MHz, DMSO— d_6): δ (ppm) 8.97 (s, 1H, N=C**H**), 8.51 (d, 1H, N—C**H**), 8.22 (d, 1H, NO_2—C—C**H**), 7.73 (t, 1H, C—C**H**), 7.33 (t, 1H, N—C=C**H**), 7.44 (d, 1H, C=C**H**) 7.59-7.88 (m, 3H, Ar-**H**-).

2.3.5. N-(2,3-dimethoxybenzylidene)pyridin-2-amine (SSSC-29)

SSSC-29 was prepared by the condensation of 2-aminopyridine with 2,3-dimethoxybenzaldehyde in methanol using glacial acetic acid as catalyst. Yield 79%, mp 232 °C, ESI–MS (*m*/*z*): 242 [M +]; ^{1}H NMR (400 MHz, DMSO— d_6): δ (ppm) 8.53 (s, 1H, N=C**H**), 8.49 (d, 1H, N—C**H**), 7.77 (t, 1H, C—C**H**), 7.28 (t, 1H, N—C=C**H**), 7.37 (d, 1H, C=C**H**) 6.89-6.99 (m, 3H, Ar-**H**-), 3.82 (s, 6H, O—C**H**$_3$).

2.3.6. N-(pyridin-3-ylmethylene)pyridin-2-amine (SSSC-30)

SSSC-30 was prepared by the condensation of 2-aminopyridine with 3-pyridinecarboxaldehyde in methanol using glacial acetic acid as catalyst. Yield 87%, mp 132 °C, ESI–MS (*m*/*z*): 183 [M +]; ^{1}H NMR (400 MHz, DMSO— d_6): δ (ppm) 8.79 (s, 1H, C=C**H**-N), 8.68 (d, 1H, N=C**H**) 8.49 (d, 1H, N—C**H**), 8.47 (s, 1H, N=C**H**), 8.13 (d, 1H, C=C—C**H**), 7.70 (t, 1H, C—C**H**), 7.37 (d, 1H, C=C**H**), 7.43 (t, 1H, N=C—C**H**), 7.28 (t, 1H, N—C=C**H**).

2.3.7. N-(anthracen-9-ylmethylene)pyridin-2-amine (SSSC-31)

SSSC-31 was prepared by the condensation of 2-aminopyridine with 9-anthraldehyde in ethanol using glacial acetic acid as catalyst. Brown crystalline solid, yield 81%, mp 110 °C, ESI–MS (*m*/*z*): 282 [M +]; ^{1}H NMR (400 MHz, DMSO— d_6): δ (ppm) 9.26 (s, 1H, N=C**H**) 8.57 (d, 1H, N—C**H**), 8.13 (d, 1H, C=C—C**H**), 7.87-8.04 (m, 4**H**, anthracene), 7.38-7.39 (m, 4**H**, Phe), 7.75 (t, 1H, C—C**H**), 7.41 (d, 1H, C=C**H**), 7.34 (t, 1H, N—C=C**H**).

2.3.8. N-benzylidenebenzo[d]thiazol-2-amine (SSSC-32)

SSSC-32 was prepared by the condensation of 2-amino-benzothiazole with benzaldehyde in ethanol using glacial acetic

acid as catalyst. Yield 81%, mp 124 °C, ESI–MS (*m*/*z*): 239 [M + H]; ^{1}H NMR (400 MHz, DMSO— d_6): δ (ppm) 8.24 (s, 1**H**, N=CH) 8.01 (dd, 2**H**, benzyl), 7.46 (dd, 2**H**, benzyl), 7.38-7.62 (m, 5**H**, phenyl).

2.3.9. 4-((benzo[d]thiazol-2-ylimino)methyl)phenol (SSSC-33)

SSSC-33 was prepared by the condensation of 2-amino-benzothiazole with *p*-hydroxy benzaldehyde in ethanol using glacial acetic acid as catalyst. Yield 81%, mp 130 °C, ESI–MS (*m*/*z*): 255 [M + H]; ^{1}H NMR (400 MHz, DMSO— d_6): δ (ppm) 9.59 (s, 1H, N=C**H**) 7.47-8.10 (m, 4**H**, benzyl), 7.37 (s, 2**H**, phenyl), 6.8 (s, 2**H**, phenyl), 4.12 (s, 1H, −O**H**); ^{13}C NMR (125 MHz, DMSO-d_6): δ (ppm) 170.106 (**C**-OH), 156.059 (**C**2-benzothiazole), 151.085 (**C**-azomethine), 149.147 (**C**8-benzothiazole), 143.018 (**C**9-benzothiazole), 140.210 (**C**6-pyridine), 135.142 (**C**-phenyl-benzothiazole) 131.096 (2**C**-phenyl), 124.730-128.041 (**C**-phenyl- benzothiazole), 121.490 (**C**-5 pyridine), 116.267 (2**C**- phenyl).

2.3.10. N-(2-nitrobenzylidene)benzo[d]thiazol-2-amine (SSSC-34)

SSSC-34 was prepared by the condensation of 2-amino-benzothiazole with 2-nitrobenzaldehyde in ethanol using glacial acetic acid as catalyst. Yield 81%, mp 110 °C, ESI–MS (*m*/*z*): 284 [M + H]; ^{1}H NMR (400 MHz, DMSO— d_6): δ (ppm) 8.24 (s, 1H, N=C**H**) 8.01 (dd, 2**H**, benzyl), 7.46 (dd, 2**H**, benzyl), 7.38-7.62 (m, 5**H**, phenyl).

2.3.11. N-(2,3-dimethoxybenzylidene)benzo[d]thiazol-2-amine (SSSC-35)

SSSC-35 was prepared by the condensation of 2-amino-benzothiazole with 2,3-dimethoxybenzaldehyde in ethanol using glacial acetic acid as catalyst. Yield 81%, mp 110 °C, ESI–MS (*m*/*z*): 299 [M + H]; ^{1}H NMR (400 MHz, DMSO— d_6): δ (ppm) 8.24 (s, 1H, N=C**H**) 8.01 (dd, 2**H**, benzyl), 7.46 (dd, 2**H**, benzyl), 7.38-7.62 (m, 5**H**, phenyl).

2.3.12. N-(pyridin-3-ylmethylene)benzo[d]thiazol-2-amine (SSSC-36)

SSSC-36 was prepared by the condensation of 2-amino-benzothiazole with 3-pyridyl carboxaldehyde in ethanol using glacial acetic acid as catalyst. White crystalline solid, yield 81%, mp 110 °C, ESI–MS (*m*/*z*): 239 [M +]; ^{1}H NMR (400 MHz, DMSO— d_6): δ (ppm) 8.71 (s, 1H, N=C**H**), 8.47 (s, 1H, C—C**H**-C in ring), 7.40-8.03 (m, 12**H**, 3 phe).

2.3.13. N-(anthracen-9-ylmethylene)benzo[d]thiazol-2-amine (SSSC-37)

SSSC-36 was prepared by the condensation of 2-amino-benzothiazole with 9-anthraldehyde in ethanol using glacial acetic acid as catalyst. Yield 81%, mp 113 °C, ESI–MS (*m*/*z*): 339 [M + H]; ^{1}H NMR (400 MHz, DMSO— d_6): δ (ppm) 8.71 (s, 1H, N=C**H**), 8.47 (s, 1H, C—C**H**-C-anthracene), 7.40-8.03 (m, 12**H**-phe).

2.4. Pharmacological screening

2.4.1. Antioxidant study by DPPH method

The free radical scavenging activity was measured by 1, 1-diphenyl-2-picryl-hydrazyl (DPPH) assay using the method described by Blois [12,13].

About 0.3 mM DPPH solution was prepared and added to 1 mL of the DPPH solution, 3 mL of the test drug solutions were added, which were dissolved in 100% methanol at different concentrations (50–250 μg/ml). The mixture was vigorously shaken and kept at room temperature in the dark for 20 min, and the absorbance was measured at 517 nm using a UV spectrophotometer. The antioxidant activity of the synthesised drugs was expressed as IC_{50} values. The IC_{50} value was defined as the concentration (μg/ml) of extracts that inhibits the formation of DPPH radicals by 50%. All tests were carried out in triplicates.

$$DPPH\ \ Scaven\,ged\ \ (\%) = \frac{A_C - A_t}{A_C} \times 100$$

where, A_c is the absorbance of the control (control containing all reagents except the test compound), A_t is the absorbance of test drugs (synthesised drugs) at different concentrations.

Concentration allowing 50% inhibition (IC_{50}) was calculated from the graph plotted by considering inhibition percentage against various concentrations and the linear regression analysis equation was used to obtain the IC_{50} value.

2.4.2. Anti-HCC screening using DEN-induced HCC rat model

2.4.2.1. Experimental animals. Male Wistar rats weighing between 250 and 350 g were procured from the Animal House, Birla Institute of Technology, Mesra, Ranchi, Jharkhand, India. The whole study was performed here in controlled conditions of temperature 24 ± 2 °C, relative humidity 50–56% and photo schedule 12 h: 12 h of light: dark. Animals were fed a standard pellet diet (Amrut Feeds, Mumbai, India) and water ad libitum. The animals were acclimatised to the laboratory conditions for one week before the initiation of the experiment. The experiments were carried out in accordance with the guidelines set by CPCSEA (Committee for the purpose of control and supervision of experiments on animals), India. The experimental design was approved by the institutional animal ethics committee of Department of Pharmaceutical Sciences and Technology, BIT, Mesra (approval No. BIT/PH/IAEC/01/2015 dated 07/07/15).

2.4.2.2. Hepatocarcinogenesis induction and treatment protocol. The experimental hepatocarcinogenesis was initiated by DEN and promoted by CCl_4 in rats as described by Farber et al. [14], Pound et al. [16] and Yadav et al. [15] with some modification. Briefly, rats (except control group I) were subjected to partial hepatectomy (PH) and administered with DEN (200 mg/kg b.w., i.p) after 24 h of stabilisation. Phenobarbital (PB, 0.05% w/v, P.O) was given to the animals for up to four weeks through drinking water. Rats were subjected to CCl_4 administration (1 mL/kg b.w, s.c) twice a week during the second and third week of pH for the promotion of carcinogenesis and left for cancer development up to Week 6. After six weeks, induced animals (six animals each) in Groups III to VIII were treated with test compounds and group II with 0.5% carboxymethylcellulose (CMC) for two weeks (Fig. 4).

2.4.2.3. Treatment regimen. Rats were randomly divided into four groups (n=6). The entire grouping was as follows:

Group I: Control; animals without any treatment or induction;

Group II: Induced control; animals induced with HCC by DEN administration as described above;

Group III: SSSC-33 LD (70 mg/kg bw, i.p); Induced animals treated with low dose (LD) of SSSC-33 from Weeks 7 to 8;

Group IV: SSSC-33 HD (140 mg/kg bw, i.p); Induced animals treated with high dose (HD) of SSSC-33 from Weeks 7 to 8.

Rats in all groups were starved overnight, anaesthetized and killed by cervical decapitation eight weeks after pH for histological and biochemical analyses. Serum was separated from the blood and used for the analysis of biochemical parameters. The liver tissue was excised immediately, rinsed in ice-cold saline and stored the frozen tissue for further histological and molecular level investigations.

2.4.2.4. Sample preparations. The liver tissue was excised immediately after killing, rinsed in ice-cold phosphate buffer saline (PBS), weighed and observed morphologically and divided

into two portions. One portion was immediately fixed in 10% formalin for histopathological examination. The remaining part of the liver was homogenised (at 20,000 rpm for 10 min) in cold PBS (pH 7.4) by using glass homogenizer tube to get tissue homogenate. Collected blood samples were centrifuged (at 3000 rpm for 15 min) to obtain serum. The serum and tissue homogenate were used for the biochemical assays.

2.4.2.5. Biochemical examination

2.4.2.5.1. Hepatic markers of liver damage and cancer. Hepatic markers enzyme activity was measured both in serum and liver tissue homogenate. Activities of aspartate aminotransferase (AST), alanine aminotransferase (ALT), alkaline phosphatase (ALP) and gamma glutamyl transpeptidase (GGT) were measured spectrophotometrically using Shimadzu recording spectrophotometer (UV–vis 1800). The ALT and AST were estimated colorimetrically as μmoles of pyruvate liberated/min/mg of protein by the method described by Huang et al. [29], ALP was measured as μmoles of phenol liberated/min/mg of protein by the method illustrated by King and Armstrong [30] and GGT was measured as μmoles of *p*-nitroaniline was formed/min/mg of protein by the method given by King [31].

Alpha-fetoprotein (AFP) is produced by the fetal liver and is used as a marker for hepatic carcinoma. AFP was determined in serum by enzyme immunoassay method using a commercial kit (Calbiotech) and following their protocol [32].

2.4.2.5.2. Enzymatic and non-enzymatic antioxidant activity. Enzymatic antioxidants like Superoxide Dismutase (SOD) and Catalase (CT) and non-enzymatic antioxidants like Glutathione (GSH) & Glutathione S-transferase (GST) levels were determined to confirm the antioxidant potential of the compound.

SOD enzymic activity determination was based on the principle of nitroblue tetrazolium (NBT) reduction described by Rukmini et al. [33]. The optical density of blue coloured formazan was taken at 560 nm by UV–vis spectrophotometer (Shimadzu UV–vis 1800). Tubes containing all reaction mixture except tissue sample serve as blank. Each unit of enzyme activity defined as the amount of enzyme required to inhibit the 50% reduction of NBT under specified condition.

CT activity was analysed by utilising the method described by Sinha et al. [34]. In this process, the level of chromic acetate formed from the reduction of dichromate in acetic acid in the presence of hydrogen peroxide (H_2O_2) determined calorimetrically at 570 nm. Catalase endogenously converts two H_2O_2 molecules to two water and one oxygen molecule. So the amount of chromic acetate indirectly reflects the amount of catalase in the sample.

GSH content in the sample was determined using the method of Van Dooran et al. [35]. The principle behind the GSH determination method is the reaction of Ellman's reagent (5,5′ bis-[2-nitrobenzoic acid]) with thiol groups of reduced GSH at pH 8.0 to produce the yellow 5-thiol-2-nitrobenzoate anion (determined calorimetrically at 412 nm). The precipitate formed by the addition of 1.0 mL of TCA to 1.0 mL of the sample was centrifuged at 1200*g* for 20 min to convert all the GSH to reduced form. The supernatant thus produced contains reduced GSH and was used for the analysis.

GST activity was determined according to the method of Habig et al. [36]. In this assay, GST catalyses the conjugation of GSH with 1-chloro-2,4-dinitrobenzene, producing a chromophore at 340 nm. The activity of GST was expressed as moles of 1-chloro-2,4-dinitrobenzene-glutathione conjugate formed min/mg of protein.

2.4.2.5.3. Determination of lipids and lipoprotein level. The level of triglycerides (TG) in plasma and hepatic tissues were estimated by the method of Van Handel [37] with small modifications done by Kumar and co-workers [38]. Total cholesterol (TC) was determined according to the method given by Parekh and Jung [39]. The level of High Density Lipoprotein Cholesterol (HDL-c), Low Density Lipoprotein Cholesterol (LDL-c), and Very Low Density Lipoprotein Cholesterol (VLDL-c) was determined through the colorimetric enzymatic (at 505 nm) method given by Sujatha and Sachdanandam [40] using HDL-c kit (Span Diagnostics Ltd., Surat, India).

2.4.2.6. Histopathological assays. The buffered formalin (10% v/v formaldehyde in PBS, for 24 h) fixed portion of the liver tissues followed through the process of dehydration using 70% v/v isopropyl alcohol (IPA). After proper dehydration, confirmed by using Xylene (clearing), tissues were impregnated in paraffin wax for 1 h at 58–60 °C (temperature should not be increased more than 65 °C) in paraffin bath and prepared paraffin blocks. The blocks were then sectioned in pieces of 4–6 μm size using rotary microtome. The sections were mounted on the slide, deparaffinized, rehydrated and stained using Hematoxylin and Eosin (H&E) stain. Finally, slides were dehydrated, put a cover slip and observed under LEICA DME microscope with Zoom Browser EX remote shooting software with appropriate magnification as required (4×, 10×, 40× and 100×).

2.4.2.7. Data analysis and statistics. Statistical analysis was carried out using Graph Pad Prism *v*6.0 (Graph Pad Software, San Diego, CA, USA). All the *in vitro* DPPH assay have been conducted in triplicate and expressed as mean ± standard error of the mean (SEM). All the in-vivo values were expressed as mean ± SEM of data obtained from six animals per group and were statistically analysed by one-way analysis of variance (ANOVA) followed by Bonferroni's multiple comparison tests with equal sample size. The difference was considered statistically significant when p value is less than (<) 0.05.

3. Results and discussion

3.1. Molecular design, and ADMET prediction

Early in-silico ADME screening and pharmacokinetic (PK) profiling provide a basis for choosing new molecular entities and lead compounds that have desirable drug metabolism, PK or safety profile, necessary selection of drug candidates and late-stage preclinical and clinical development. The molecular designing approach in early drug development process helps to select ligand molecules having good ADME property from a large lot and reduces unnecessary cost on the irrelevant ligands. In the past, many ligands were discarded in the later stage of drug discovery due to inappropriate PK and pharmacodynamics (PD) properties [41]. So it is very necessary to consider PK and PD parameters in the early stage of drug development [42]. Molecular modelling supports drug discovery process by producing ligands with satisfactory PK and PD parameters so that the resulted molecules will probably give good activity regarding disease concerned with good PK and PD properties.

The primary aim of any new drug discovery is to develop orally active drugs. Lipinski's Rule of 5 (Ro5) [43] states that orally active molecules have a molecular weight (MW) below 500D, hydrogen bond acceptor (HBA) groups below 10, hydrogen bond donor (HBD) groups below 5 and oil/water partition coefficient (logPo/w) below 5. We utilised Rule of five (RO5) as a rule of thumb to evaluate drug-likeness or determine if a chemical compound with a certain pharmacological or biological activity has properties that would make it a likely orally active drug in humans. All the designed molecules obeyed Ro5 parameters (Table 3), indicates that all

Table 3
Lipinski Rule of Five analyses of the compounds.

Serial No.	Comp.	"Rule of Five"			
		Mol.Wt[a]	HBA[b]	HBD[c]	QPlogPo/w[d]
1	SSSC-26	168.21	2	0	3.091
2	SSSC-27	225.26	3	1	2.41
3	SSSC-28	282.32	3	0	2.48
4	SSSC-29	360.45	4	0	3.34
5	SSSC-30	239.29	4	0	2.03
6	SSSC-31	296.34	2	0	4.93
7	SSSC-32	324.40	2	0	3.53
8	SSSC-33	271.35	3	1	3.08
9	SSSC-34	360.45	4	0	3.13
10	SSSC-35	360.45	4	0	3.94
11	SSSC-36	328.40	4	0	2.69
12	SSSC-37	443.49	3	0	5.58
13	Sorafenib	464.82	6	3	4.09

[a] Molecular weight.
[b] Hydrogen bond acceptor.
[c] Hydrogen bond donor.
[d] Predicted octanol/water partition coefficient.

compounds are more apt to be membrane permeable and easily absorbed by the body [44].

In this study, all the designed molecules were analysed in-silico using QikProp module of Schrodinger software suite *v*8.5 to establish their PK parameters (Table 4). The descriptors like QPPCaco, QPlogS, the percentage of oral absorption, dipole moment, PlogBB, SASA and QplogKhsa were analysed [45]. Cell permeability of the designed molecules was determined regarding QPPCaco. The results depicted that molecules SSSC-26 to SSSC-37 have QPPCaco values greater than 500 nm/s and which shows that these molecules have better cell permeability than sorafenib (a multi-kinase inhibitor approved for HCC treatment). The sufficient number of hydrophilic-lipophilic groups may be the reason for their high cell permeability. The percentage of oral absorption of all the molecules are 100. The predicted aqueous solubility (QPlogS) and solvent-accessible surface area (SASA) of the compounds were in the accepted range of −6.235 and −2. 036 and 300–1000 respectively, which are sufficiently useful for the oral activity.

The fraction bound to human serum albumin acts as reservoir and releases as the concentration in the plasma reduces through elimination. Prediction of binding to human serum albumin (QPlogKhsa) was shown that SSSC-31 to 35 and SSSC-37 have higher values than others. So these molecules can be considered for extended release of action. The central nervous system (CNS) toxicity profile was determined by predicting brain/blood partition coefficient (PlogBB). The data justifies that none of the molecules can cross the blood-brain barrier to producing CNS toxicity.

3.2. Molecular docking studies

The main aim of docking study was to establish the multi-receptor interaction of the designed ligands to counter the drug resistance. As in the case of Sorafenib, a multikinase inhibitor, the development of drug resistance can be overcome through the discovery of medicines having multiple receptor activities. In the case of HCC chek1 and EGFR receptors are overexpressed and so utilised in this study to carry out docking simulation using Glide *v*5.0 of Schrodinger software suite *v*8.5.

Chk1 is responsible for directing cellular mechanism to repair damaged DNA and which is the only repairing mechanism available for HCC cells since all the other mechanisms were mutated during the HCC formation. Through the inhibition of Chk1 receptor, the entire damaged DNA repairing mechanism will be stopped and damaged cells undergoes apoptosis. Similarly, VEGFR is responsible for the angiogenesis in HCC and is overexpressed. Continued tumour expansion in HCC occurs with the production of new blood vessels (angiogenesis). Anti-angiogenic effect of the compounds and thus anti-HCC activity can be established by the EGFR inhibition.

Docking studies were started with the ligand preparation utilising LigPrep, protein preparation employing Prep Wizard and receptor grid generation. All these processes are necessary to meet minimum requirements for molecular docking calculation. In ligand preparation, optimisation and energy minimization of designed ligands were carried out. After ligand preparation, the downloaded receptors (Chk1, 1ZYS; VEGFR, 2QU5) from PDB (Figs. 2 and 3) were refined (protein preparation) to include missing side chain, remove water molecules which are not having interaction, adjust formal charges of the atoms of the protein and metal ion associated and to correct the ionisation and tautomerization state of the protein.

All the 12 designed molecules (SSSC-26 to 37) and sorafenib were docked into the active site of Chk1 and VEGFR-2 using Glide *v*5.0. The Glide score (G-score) thus obtained were tabulated in Table 5. The validation of docking program was done by re-docking method. The low root mean square deviation (RMSD) value indicates the docking method has better ability to reproduce the X-ray bound confirmation for the receptors, Chk1 and VEGFT-2.

The G-scores of the test compounds against Chk1 were found in between −5.13 and −6.44 Kcal/mol and against VEGFR-2 were

Table 4
Predicted pharmacokinetic properties using QikProp module of Schrodinger software suite *v*8.5.

Serial No.	Comp.	QPP Caco[a]	QPlogS[b]	% of Oral Abso.	Dipole Moment	PlogBB[c]	SASA[d]	QPlog Khsa[e]
1	SSSC-26	4704.2	−2.958	100	**	0.083	436.724	−0.021
2	SSSC-27	1425.3	−2.847	100	**	−0.469	449.111	−0.118
3	SSSC-28	927.8	−2.864	100	**	−0.645	468.033	−0.133
4	SSSC-29	6239.5	−3.172	100	**	0.069	506.684	−0.068
5	SSSC-30	2548.3	−2.036	100	**	−0.161	429.532	−0.462
6	SSSC-31	5071.3	−5.210	100	**	0.096	555.609	0.727
7	SSSC-32	3920.5	−3.599	100	**	0.093	476.481	0.125
8	SSSC-33	1376.8	−3.892	100	**	−0.429	507.627	0.089
9	SSSC-34	878.9	−3.900	100	**	−0.627	527.506	0.063
10	SSSC-35	5720.7	−4.089	100	**	0.120	559.856	0.115
11	SSSC-36	2542.9	−3.038	100	**	−0.096	487.451	−0.270
12	SSSC-37	4864.1	−6.235	100	**	0.143	615.789	0.927
13	Sorafenib	333.48	−6.900	96.06	6.0	−0.929	759.72	0.324

[a] Predicted apparent Caco-2 cell (the model for the gut blood brain barrier) permeability in nm/s (<25 poor > 500 great).
[b] Predicted aqueous solubility (−6.5–0.5); S in moldm^{-3}.
[c] Predicted brain/blood partition coefficient (−3–1.2).
[d] Total solvent accessible surface area in square angstrom (300–1000).
[e] Prediction of binding to human serum albumin (−1.5–1.5).
** Data not available.

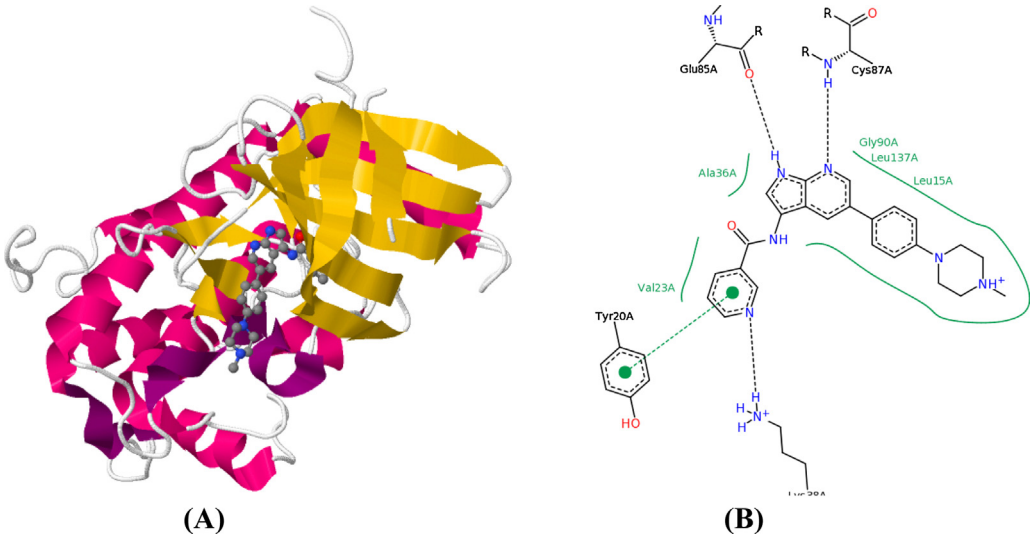

Fig. 2. (A): Co-crystal structure of Checkpoint Kinase 1 (Chk1) (PDB: 1ZYS) with a pyrrolo-pyridine inhibitor. (B): 2D Pose view of N-[5-[4-(4-Methylpiperazin-1-yl)phenyl]-1h- pyrrolo[2,3-*b*]pyridin-3-yl] nicotinamide in IZYS. Retrieved from protein data bank (PDB) site [20].

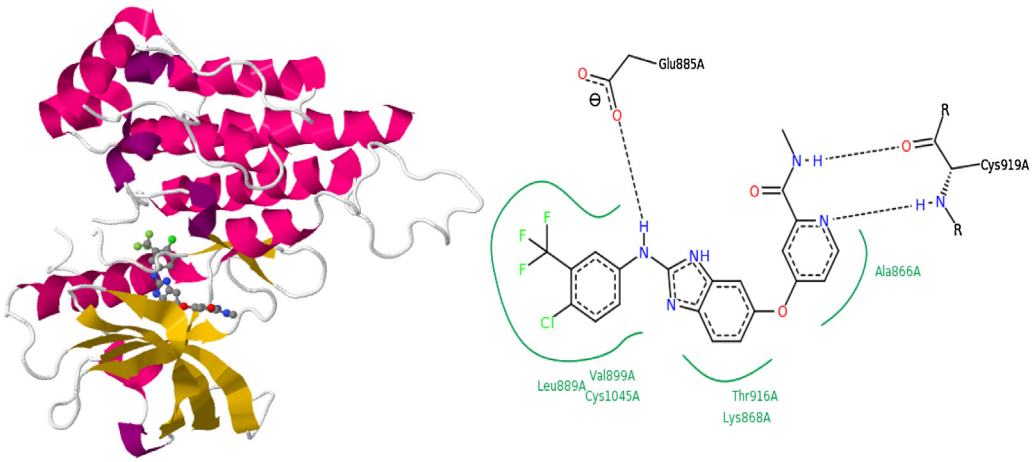

Fig. 3. (A): Crystal structure of the VEGFR2 kinase (PDB: 2QU5) domain in complex with a benzimidazole inhibitor. (B): 2D Pose view of 4-[[2-[[4-chloro-3-(trifluoromethyl) phenyl]amino]-3H-benzimidazol-5-yl]oxy]-N-methyl-pyridine-2-carboxamide in 2QU5. Retrieved from PDB site [22,23].

found in between −6.47 and −8.37 Kcal/mol. SSSC-37 and SSSC-32 were shown higher G-score towards Chk1 and VEGFR-2 protein respectively. Whereas, G-score of sorafenib was found to be −3.68 Kcal/mol against Chk1 and −10.6 Kcal/mol against VEGFR-2. The higher scoring function directly relates to the higher binding affinities. The structural features that provide hydrophobic interaction, Van Der Waals (vdW) forces, dispersion interaction, hydrogen bonding, and other electrostatic interactions between amino acids of the protein and ligand and solvation effect determine the strength of the ligand-protein binding. The 3D images of receptor-ligand interaction (Fig. 5) after docking show a sufficient number of hydrogen bonding and hydrophobic interactions to establish the inhibitory effect of the ligands on both the receptors.

3.3. In-silico acute toxicity study using ProTox

The safety of the drugs developed is one of the primary requirement for regulatory authorities for the approval for clinical use. Acute toxicity studies are performed to prove the safety of the new drug. The gap between minimum effective concentration and minimum toxic concentration (therapeutic window) should be sufficiently large. Many drugs were called back from the market and failed in the later stage of drug development due to the severe toxicity [46]. So early assessment of toxicity is necessary for the successful approval and marketing of new drugs.

Lethal Dose 50% (LD_{50}), the dose at which 50% of the tested animal die upon administration of the compound, gives insight to the level of acute toxicity. The LD_{50} values were predicted after oral administration in rodents using ProTox and are tabulated in Table 6. All the compounds showed LD_{50} values between $300 < LD_{50} \leq 2000$ mg/kg and so came under the class 4 according to the Globally Harmonized System of Classification of Labeling of Chemicals (GHS), United Nations guidelines. This clearly indicates that all these compounds are only harmful if swallowed and are safe for the development of a new drug.

3.4. Chemistry

The strategy followed in the synthesis of proposed Schiff bases (SSSC-26 to SSSC-37) are outlined in the Scheme 1. The condensation between primary amines (2-aminopyridine and 2-aminobenzothaizole) and aldehydes (benzaldehyde, *p*-hydroxybenzaldehyde, 2-nitrobenzaldehyde, 2,3-dimethoxybenzaldehyde,

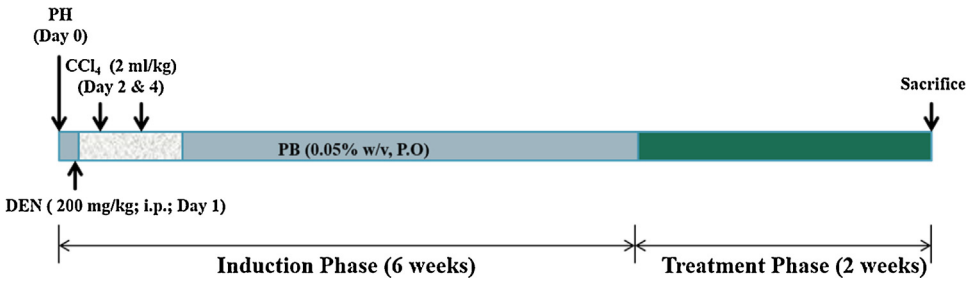

Fig. 4. Treatment protocol of the study. CCl_4-carbontetrachloride, DEN-diethylnitrosamine, i.p- intraperitoneal, PB-phenobarbitone sodium, PH-partial hepatectomy, P.O-peroral.

Table 5
Docking score generated by Glide 5.0.

Entry	Compound	Glide 5.0 Score	
		CHK1[a] receptor (PDB Id-1ZYS)	VEGFR−2[b] Kinase PDB Id−2QU5
1	SSSC-26	−6.29	−7.04
2	SSSC-27	−5.44	−6.84
3	SSSC-28	−5.44	−7.15
4	SSSC-29	−5.24	−7.08
5	SSSC-30	−5.67	−7.29
6	SSSC-31	−6.24	−6.47
7	SSSC-32	−5.13	−8.37
8	SSSC-33	−5.55	−7.87
9	SSSC-34	−5.58	−6.98
10	SSSC-35	−5.38	−7.62
11	SSSC-36	−5.21	−7.55
12	SSSC-37	−6.44	−7.32
13	Sorafenib (std)	−3.68	−10.60

[a] Checkpoint kinase1.
[b] Vascular endothelial growth factor receptor-2.

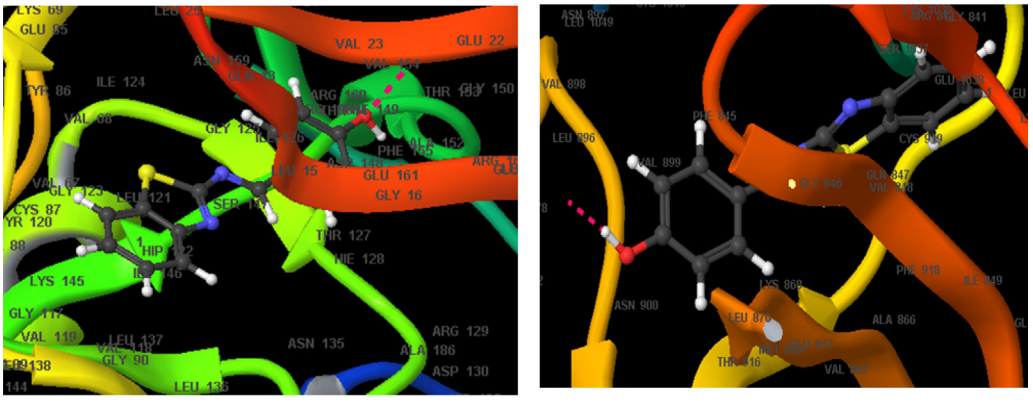

Fig. 5. (A) SSSC-33 in the active site of Chk 1 receptor (PDB ID: 1ZYS), G-score:-5.55; (B) SSSC-33 in the active site of VEGFR-2 (PDB ID: 2QU5), G-score:-7.87. The image was generated by Glide *v*5.0. Protein is depicted in the ribbon model and ligand in ball and stick model in which grey colour represents carbon (C); red, oxygen (O); blue, nitrogen (N); yellow, Sulphur (S) and white, hydrogen (H).

3-pyridylcarboxaldehyde and 9-anthraldehyde) in the presence of glacial acetic acid as catalyst methanol or ethanol as solvent yield 12 different Schiff bases in good yield. The formation of Schiff's base occurs in two separate steps; formation of carbinolamine and formation of imine (Schiff's base). The carbinolamine was converted to imine in the presence of glacial acetic acid [47]. The recrystallization of the compounds was done using a mixture of ethyl acetate and ethanol.

Characterization was carried out by elemental analysis and MASS, ^{1}H NMR, and ^{13}C NMR (SSSC-26 and SSSC-33; one each from 2-aminopyridine and 2-aminobenzo thiazole series respectively) spectroscopic methods. The mass spectrum supports the proposed empirical formula of the compound. It reveals the molecular ion peak *m*/*z* at consistent with the molecular weight of the ligand. The NMR Spectral data showed characteristic peaks relevant to the synthesised compounds and depicted in Section 2.3.

3.5. Free radical scavenging activity by DPPH method

All the synthesised compounds were subjected to free radical scavenging assay through DPPH method to find out its anti-oxidant potential. The DPPH assay is a reliable method for the evaluation of

Table 6
Predicted LD_{50} of and toxicity class of designed compounds.

SL. No.	Compound	LD_{50} mg/Kg	Toxicity class
1	SSSC-26	2000	Class IV
2	SSSC-27	2000	Class IV
3	SSSC-28	2000	Class IV
4	SSSC-29	2000	Class IV
5	SSSC-30	1500	Class IV
6	SSSC-31	2000	Class IV
7	SSSC-32	1000	Class IV
8	SSSC-33	1000	Class IV
9	SSSC-34	1000	Class IV
10	SSSC-35	562	Class IV
11	SSSC-36	1000	Class IV
12	SSSC-37	1000	Class IV
13	Sorafenib	800	Class IV

Class I: fatal if swallowed (LD50 ≤ 5 mg/kg), Class II: fatal if swallowed (5 < LD50 ≤ 50 mg/kg), Class III: toxic if swallowed (50 < LD50 ≤ 300 mg/kg), Class IV: harmful if swallowed (300 < LD50 ≤ 2000 mg/kg), Class V: may be harmful if swallowed (2000 < LD50 ≤ 5000 mg/kg), Class VI: non-toxic (LD50 > 5000 mg/kg).

antioxidant property because of its stability in the radical form and simplicity of the test [48]. The method is based on the reduction of DPPH (purple in colour) to corresponding hydrazine (yellow in colour) by receiving hydrogen atom from the anti-oxidant. The colour changes can be measured quantitatively by spectrophotometer absorbance at 517 nm [49].

The percentage of inhibition at 50, 100, 150, 200 and 250 μg/ml concentration and IC_{50} (concentration at which 50% DPPH activity inhibited) values of the synthesised compound were determined and reported (Table 7). The data was compared with the ascorbic acid (standard), a known anti-oxidant (Figs. 6 and 7). Out of 12 synthesised compounds SSSC-29 and 33 showed IC_{50} values of 63.60 μg/ml and 60.32 μg/ml respectively and which was comparable with that of ascorbic acid (IC_{50} – 55.27 μg/ml). The Higher antioxidant potential is associated with the lower IC_{50} value. So, SSSC-33 has higher DPPH scavenging property thus anti-oxidant potential among other test compounds.

3.6. Anti-HCC screening

On the basis of anti-oxidant property and docking score SSSC-33 was selected for the anti-HCC screening using DEN-induced hepatocellular carcinoma rat model. The activity was determined by comparing with the normal control (without induction and treatment) and induced control (HCC induced but not treated).

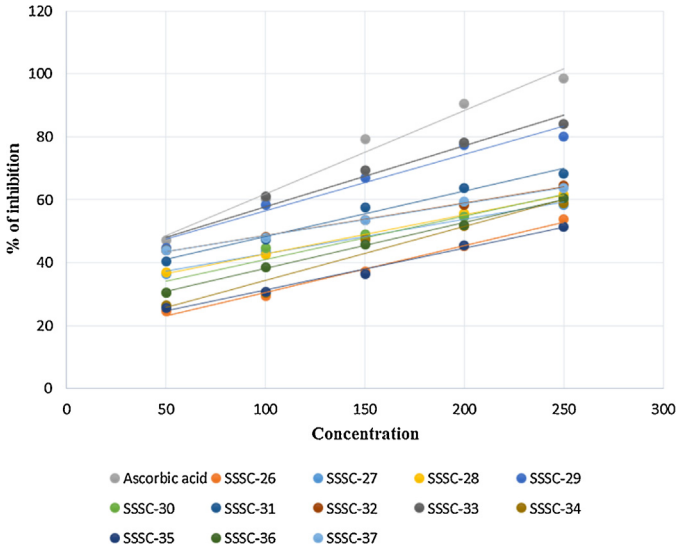

Fig. 6. The concentration versus percentage inhibition graph with linear regression line of ascorbic acid and test compounds.

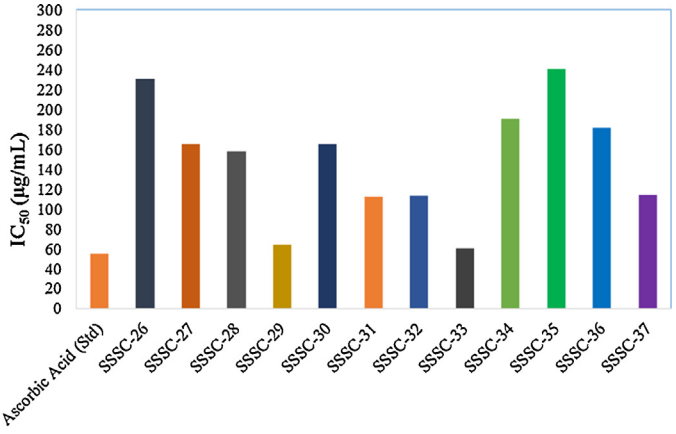

Fig. 7. Comparison of IC_{50} values of test compounds with ascorbic acid.

3.6.1. Restoration of liver function

The effect of SSSC-33 in HCC induced hepatic damage was evaluated by estimating activities of hepatic marker enzymes such as AST, ALT, ALP, and GGT both in serum and liver homogenate and level of AFP in serum. Serum activities of hepatic markers AST, ALT,

Table 7
The percentage of scavenging of DPPH radical and IC_{50} values of standard (ascorbic acid) and test compounds (SSSC-26 to SSSC-37).

Sl.No.	Compound	% Scavenging of DPPH radical					IC_{50} (μg/ml)
		50	100	150	200	250	
1	Ascorbic Acid (Std)	47.23 ± 0.36	60.27 ± 0.39	79.29 ± 0.45	90.63 ± 0.28	98.54 ± 0.25	55.27
2	SSSC-26	24.51 ± 0.26	29.32 ± 0.31	37.32 ± 0.24	45.21 ± 0.34	53.71 ± 0.41	230.64
3	SSSC-27	36.51 ± 0.15	43.71 ± 0.26	48.31 ± 0.38	54.71 ± 0.18	58.44 ± 0.16	165.20
4	SSSC-28	37.03 ± 0.51	42.51 ± 0.12	48.52 ± 0.14	55.73 ± 0.31	61.52 ± 0.24	157.52
5	SSSC-29	44.73 ± 0.32	58.33 ± 0.32	67.01 ± 0.35	77.29 ± 0.31	80.03 ± 0.15	63.60
6	SSSC-30	30.52 ± 0.44	44.79 ± 0.22	49.03 ± 0.28	54.71 ± 0.25	60.21 ± 0.19	165.50
7	SSSC-31	40.41 ± 0.25	47.37 ± 0.37	57.66 ± 0.28	63.74 ± 0.22	68.31 ± 0.06	111.94
8	SSSC-32	43.91 ± 0.21	48.31 ± 0.31	53.66 ± 0.25	58.31 ± 0.15	64.61 ± 0.35	113.42
9	SSSC-33	44.24 ± 0.13	60.99 ± 0.31	69.46 ± 0.41	78.23 ± 0.36	84.21 ± 0.33	60.32
10	SSSC-34	26.61 ± 0.71	30.51 ± 0.17	47.37 ± 0.22	51.61 ± 0.09	58.88 ± 0.24	190.87
11	SSSC-35	25.69 ± 0.58	30.77 ± 0.29	36.47 ± 0.36	45.55 ± 0.19	51.34 ± 0.31	241.00
12	SSSC-36	30.55 ± 0.26	38.51 ± 0.45	45.77 ± 0.31	51.89 ± 0.34	60.44 ± 0.33	181.24
13	SSSC-37	43.85 ± 0.65	48.01 ± 0.41	53.61 ± 0.24	59.41 ± 0.15	63.71 ± 0.14	113.68

Each value represents mean ± SEM, (n = 3); SEM-standard error of the mean.

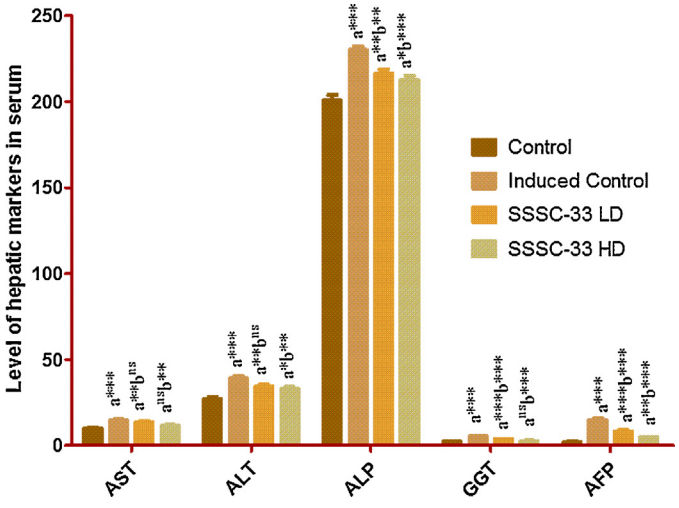

Fig. 8. Effect of SSSC-33 on hepatic markers in serum of rat with HCC. Values are expressed as mean ± SEM of six rats per group; where, a- Group II, III, IV compared with Group I; b- Group III & IV compared to Group II; $^{***}p < 0.001$; $^{**}p < 0.01$; $^{*}p < 0.05$; $^{ns}p > 0.05$; Group I- Normal Control; Group II- Induced Control; Group III- treated with SSSC-33 LD; Group IV- treated SSSC-33 HD. AST-aspartate aminotransferase, ALT-alanine transferase, ALP-alkaline phosphatase, GGT-gamma glutamyl transferase, AFP-alpha fetoprotein.

ALP, and GGT and level of AFP were increased significantly ($p < 0.001$) in Group II as compared to control rats (Group I), thus indicating liver damage (Fig. 8). On the other hand, the activity of AST and ALT was significantly ($p < 0.001$) decreased, and the activity of ALP and GGT was significantly ($p < 0.001$) increased in the liver tissue of animals from Group II as compared with Group I (Fig. 9). The low dose of SSSC-33 was restored hepatic marker enzymes activity less significantly whereas the high dose restored the activity of AST ($p < 0.01$), ALT ($p < 0.01$), ALP ($p < 0.001$), GGT ($p < 0.001$), and AFP ($p < 0.001$) in serum on comparison with induced control (Group II) significantly. In the case of liver homogenate of rats from Group IV (rats treated with SSSC-33 HD) the activity of AST ($p < 0.001$), and ALT ($p < 0.001$) was increased significantly, and the activity of ALP ($p < 0.001$), and GGT ($p < 0.001$) was decreased significantly compared with rats from the induced control group. This indicates that SSSC-33 HD can revoke the changes happened in the liver functions of rats induced

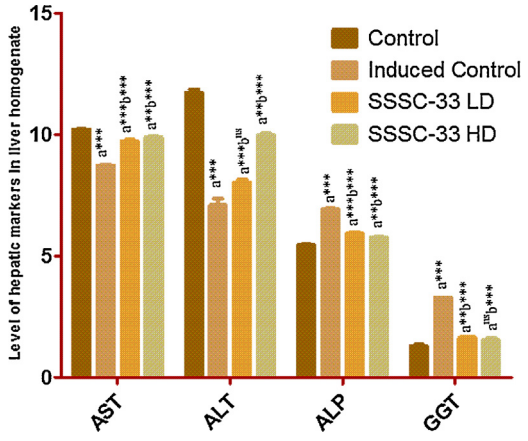

Fig. 9. Effect of SSSC-33 on hepatic markers in liver homogenate of rats induced with HCC. Values are expressed as mean ± SEM of six rats per group; where, a- Group II, III, IV compared with Group I; b- Group III & IV compared to Group II; $^{***}p < 0.001$; $^{**}p < 0.01$; $^{*}p < 0.05$; $^{ns}p > 0.05$; Group I- Normal Control; Group II- Induced Control; Group III- treated with SSSC-33 LD; Group IV- treated SSSC-33 HD. AST-aspartate aminotransferase, ALT-alanine aminotransferase, ALP-alkaline phosphatase, GGT-gamma-glutamyltransferase.

with HCC by DEN injection. These results coincide with the observations obtained by Jahan et al. [50].

Assessment of hepatic function is essential to monitor HCC progression and prognosis and the effect of anti-cancer drugs. Hepatic marker level significantly alters in the case of cancer induction. Increase transaminase activities in HCC have been reported by Rochi et al. [51] ALP and AST are considered as a most sensitive tumour marker for malignant diseases. The increased serum activity of AST and ALT in HCC induced group was due to the presence of high cancerous cells and thereby high liver marker enzyme synthesis [52]. ALP is involved in the transport of metabolites across the cell membrane, protein synthesis, secretory activities and glycogen metabolism. The rise in an activity of ALP in DEN-induced HCC animals may be due to the disturbance in the secretory activity and altered synthesis of the enzyme [53]. An increase in GGT activity paralleled with an increase in ALP activity is very common in HCC [54]. α-feto protein (AFP) is a serum protein is detected in elevated concentration in conditions like HCC. It is size, structure and composition are similar to serum albumin, but is detectable in minute quantities in normal condition. Elevated serum concentration is specifically observed in HCC [50]. So its serum concentration can be used to confirm HCC and for the diagnosis of tumour response therapy. Here in this study, the elevated level of AFP in DEN-treated group (Group II) was significantly restored towards normal level in Group IV (SSSC-33 HD treated), which indicates clearly suggests the anti-HCC potential of SSSC-33.

3.6.2. Effect of SSSC-33 on the level of enzymic and non-enzymic antioxidants

The *in vitro* antioxidant property of SSSC-33 was detected by the DPPH method. Further, it was confirmed by measuring levels of enzymic antioxidants in both liver homogenate and serum and non-enzymic antioxidants in serum and is summarised in Tables 8 and 9. Group II (induced control) animals exhibited significant increase ($P < 0.001$) in GSH level and GST activity and a decrease in SOD and CAT activities compared to Group I (normal control). These findings are consistent with the hepatic oxidative stress and damage caused by DEN. The high dose of SSSC-33 ($p < 0.001$) increases the level of SOD and CAT and decreases the level of GSH and activity of GST towards normal in comparison with Group II.

Endogenously, a dynamic equilibrium between generated free radicals and antioxidant defence system exists that protects from deleterious effects of oxidative damage. During oxidative stress, like in cancer, this equilibrium disrupts, and the level of enzymic antioxidants like SOD and CAT decreases due to the over usage to act against free radicals. GSH, a tripeptide, act as intracellular anti-oxidant and protects from free radical induced cellular damage and produce a substrate for GST and other anti-oxidant enzymes. The increased level of GSH and increased GST activity in Group II clearly indicates the over production of these enzymes due to increased level of ROS occurred in hepatocarcinogenesis. So, the anti-cancer potential of any drug can be assessed by screening the level of these enzymic and non-enzymic antioxidants. The anti-cancer potential of SSSC-33 established through the reversal of SOD, CAT and GST towards normal level (normal control).

3.6.3. Lipids and lipoprotein evaluation in plasma

The level of lipids and lipoprotein were evaluated as described to get additional information for a complete assessment and monitoring of the liver function with HCC and results obtained are depicted in Fig. 10. The data showed that the level of TC, TG, LDL, and VLDL was significantly ($p < 0.001$) increased and the level of HDL ($p < 0.001$) significantly decreased in the plasma sample of rats from Group II as compared with Group I. This clearly indicates the development of cancerous tissue in response with DEN. SSSC-

Table 8
Effect of SSSC-33 on the level of enzymic antioxidants in HCC induced animals.

	SOD (units/mg of protein)		CAT (μmol of H_2O_2 consumed/min/mg of protein)	
	Serum	Liver	Serum	Liver
Group I	8.77 ± 0.153	5.05 ± 0.16	61.76 ± 0.25	31.32 ± 0.29
Group II	4.56 ± 0.22a***	2.07 ± 0.05 a***	40.24 ± 0.21 a***	19.19 ± 0.19 a***
Group III	5.69 ± 0.213a***b^{ns}	3.40 ± 0.03 a***b***	44.39 ± 0.21 a***b*	21.24 ± 0.92 a***b^{ns}
Group IV	6.91 ± 0.33a***b***	4.55 ± 0.20 a*b***	46.95 ± 0.22 a***b***	22.26 ± 0.61 a***b***

Values are expressed as mean ± SEM of six rats per group; where, a- Group II, III, IV compared with Group I; b- Group III & IV compared to Group II; Group I- Normal Control; Group II- Induced Control; Group III- treated with SSSC-33 LD; Group IV- treated with SSSC-33 HD. SOD-superoxide dismutase, CAT-catalase.
$^{**}p < 0.01$.
$^{*}p < 0.05$.
$^{***}p < 0.001$.
$^{ns}p > 0.05$.

Table 9
Effect of SSSC-33 on the level of non-enzymic antioxidants in liver of HCC induced animals.

	GSH (μg/mg of protein)	GST (unit/mg protein)
Group I	2.85 ± 0.04	391.58 ± 1.12
Group II	3.27 ± 0.02 a***	786.52 ± 0.80 a***
Group III	3.11 ± 0.04 a***b**	774.02 ± 3.21 a***b**
Group IV	3.08 ± 0.05 a***b***	612.45 ± 2.58 a***b***

Values are expressed as mean ± SEM of six rats per group; where, a- Group II, III, IV compared with Group I; b- Group III & IV compared to Group II; $^{***}p < 0.001$; $^{**}p < 0.01$; $^{*}p < 0.05$; $^{ns}p > 0.05$; Group I- Normal Control; Group II- Induced Control; Group III- treated SSSC-33 LD; Group IV- treated with SSSC-33 HD. GSH-glutathione, GST-glutathione-S-transferase.

33 treated groups showed a decrease in TC, TG, LDL and VLDL and increased in HDL towards normal control group. The SSSC-33 HD had given significance difference from induced control to normal control values. The reestablishment of lipids and lipoprotein level in the plasma with the treatment with SSSC-33 indicates its anti-cancer effect in HCC, but the effect significantly differed from the control group. As the liver plays a crucial role in lipid and lipoprotein metabolism, the significant impairment of the hepatic function occurring during chronic liver diseases, such as HCC, can influence plasma lipoprotein profiles. There is always a major change found in the levels of lipoproteins along with TC and TG with patients with HCC [55].

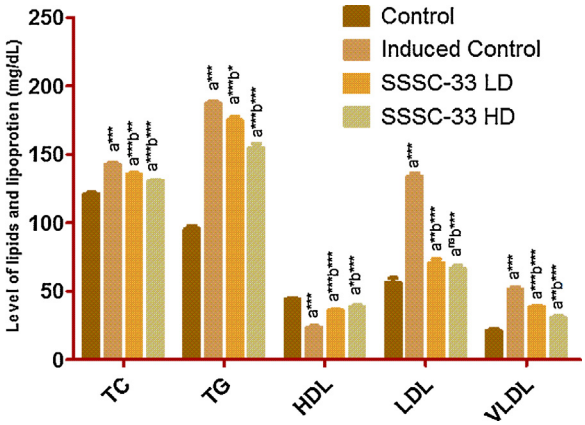

Fig. 10. Effect of SSSC-33 on lipids and lipoprotein in plasma of rat induced with HCC. Values are expressed as mean ± SEM of six rats per group; where, a- Group II, III, IV compared with Group I; b- Group III & IV compared to Group II; $^{***}p < 0.001$; $^{**}p < 0.01$; $^{*}p < 0.05$; $^{ns}p > 0.05$; Group I- Normal Control; Group II- Induced Control; Group III- treated with SSSC-33 LD; Group IV- treated SSSC-33 HD. LC-total cholesterol, TG-triglycerides, HDL-high density lipoprotein, LDL- low-density lipoprotein, VLDL-very low-density lipoprotein.

3.6.4. Effect of SSSC-33 on liver weight and histopathological investigation of liver sections

On completion of eight weeks, all the animals were sacrificed and examined the liver weight (Table 10). It was observed from the data that cancer induction causes an overall increase in liver weight due to the presence of a tumour. Liver regains its normal weight after the treatment with SSSC-33 HD ($p < 0.01$) in comparison with induced control (Fig. 11).

The histological examination of the liver tissue of all groups by hematoxylin and eosin staining is shown in Figs. Fig. 12C&D and Fig. 13C&D. In the normal control group the section showed cells with intact architecture with normal nuclei, but the liver sections of HCC rats (Group II), showed loss of architecture, the presence of binucleate, enlarged, polygonal hepatocytes with acidophilus staining cytoplasm. The DEN-treated groups also showed irregular sinusoids and degenerated tumour cells. Some cells in DEN-treated liver tissue exhibited multiple proliferating nucleoli, and some cells possess intranuclear vacuole or cytoplasmic vacuoles. A massive area of vacuolated hepatocytes, cellular infiltration, pyknotic nuclei, and Numerous Kupffer cells was found.

The histopathological investigation of the rats treated with SSSC-33 (Group III&IV) showed cells with architecture more or less like the control one. The sinusoids were regularised in greater extent in Group IV compared with Group III.

4. Concluding remarks

In this study we were tried to develop new azomethine based lead compound having multi-receptor action on HCC like sorafenib through molecular modelling, synthesis and pharmacological screening. Twelve different azomethine compounds based on 2-aminopyridine (SSSC-26 to 31) and 2-aminobenzothiazole (SSSC-32 to 37) were designed. The pharmacokinetic evaluation using QikProp showed that all compounds have sufficient structural features to develop as an oral drug. Further, Ro5 analysis proved that compounds were having all the parameter required for the oral activity. Acute toxicity studies using ProTox web server revealed LD_{50} values (500–2000 mg/kg, b.w) of each compound and showed that these molecules are safe enough to apply as a drug. The docking score of the compounds was satisfactory enough to explain the ability of the compounds to bind with VEGFR, and Chk1 receptor to elicit anti-HCC action. After molecular modelling

Table 10
The effect of SSSC-33 on liver weight of rats induced with HCC.

Groups	Liver weight in Grams
Group I (Normal control)	7.54 ± 0.15
Group II (Induced control	9.67 ± 0.22a***
Group III (SSSC-33 LD treated)	9.02 ± 0.28a***b^{ns}
Group IV (SSSC-33 HD treated)	8.37 ± 0.14a^{ns}b**

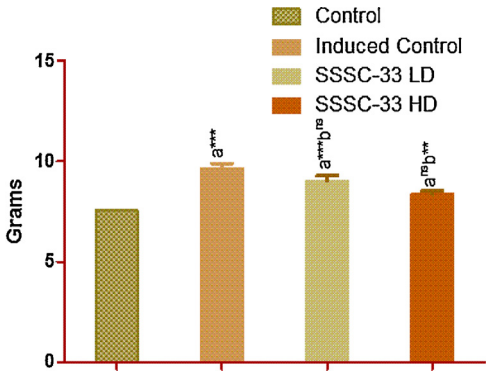

Fig. 11. The effect of SSSC-33 on the liver weight of rats induced with HCC. Values are expressed as mean ± SEM of six rats per group; where, a- Group II, III, IV compared with Group I; b- Group III & IV compared to Group II; ***$p < 0.001$; **$p < 0.01$; *$p < 0.05$; $^{ns}p > 0.05$; Group I- Normal Control; Group II- Induced Control; Group III- treated with SSSC-33 LD; Group IV- treated SSSC-33 HD.

leads were synthesised and characterised by different spectroscopic methods. The results thus obtained proved the structural integrity of the compounds.

We evaluated DPPH scavenging property of all compounds, SSSC-29 and SSSC-33 showed lowest IC_{50} values of 63.60 and 60.32 respectively and showed significant antioxidant potential in comparison with ascorbic acid (IC_{50}- 55.27), a known antioxidant.

The anti-HCC evaluation of SSSC-33 in DEN (200 mg/kg, bw) induced rat model was carried out and determined level of hepatic markers, enzymic and non-enzymic antioxidants, examined histopathological slides of liver and compared statistically with the respective data of induced control and normal control.

The elevation of hepatic markers like AST, ALT, ALP and GGT in serum was observed in cancer-induced groups as previously reported due to the overproduction and membrane damage and confirms the HCC induction. On the contrary, SSSC-33 HD treatment in Group IV resulted in a significant reversal of altered level of hepatic markers to control values which are a sign of the liver improvement to a normal state. The antioxidative defence system of the body scavenges ROS that helps in the initiation of lipid peroxidation and, therefore, plays a protective role in cancer development. This protection system operates through enzymatic (SOD and CAT), and non-enzymatic (GST and GSH) components. In the present study, the decreased activity of SOD, CAT, GSH and GST in liver found in HCC rats was restored SSSC-33 HD towards normal value. The elevation in the level of enzymatic and nonenzymatic antioxidants may be due to the ability of SSSC-33 to prevent ROS formation. Finally, comparison of histopathological changes and liver weight variation of animals in Group IV with Group II further confirms the anti-HCC potential of SSSC-33.

Thus SSSC-33-((benzo[d]thiazol-2-ylimino)methyl)phenol), appeared to be effective free radical scavenger with antioxidant activities. Also, it could protect rat liver from DEN-induced altered hepatic functioning, and prevent further progression through the inhibition of Chk1and VEGFR-2. Furthermore, from all the above mentioned overwhelming results it can be concluded that Schiff's' base prepared from 2-aminopyridine like SSSC-33 is a potential anti-cancer therapeutic agent and an appropriate candidate for further development as an anti-HCC agent. Also, it is necessary to improve the anti-HCC property of SSSC-33 without hampering the pharmacokinetic and toxicological profile.

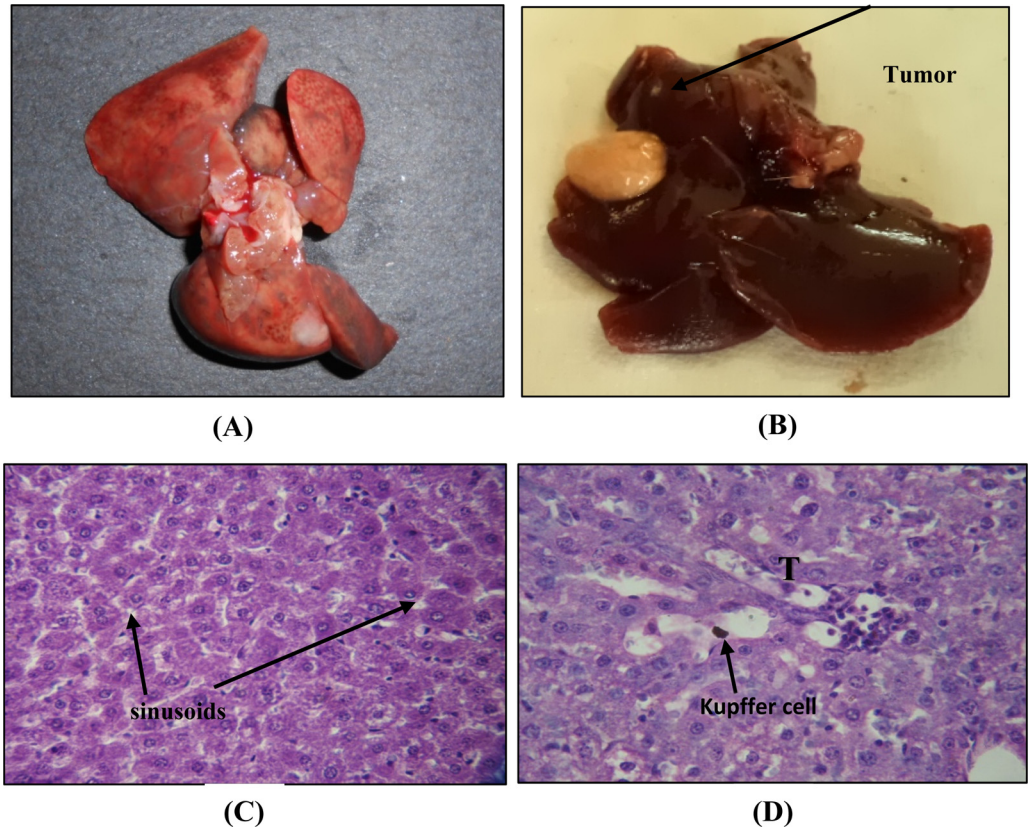

Fig 12. A&B morphological views of normal liver (Group I) and HCC induced liver (Group II) respectively; C&D Hematoxylin and Eosin stained liver tissue of normal liver and HCC induced liver respectively observed under LEICA DME microscope (40×). T-tumour tissue.

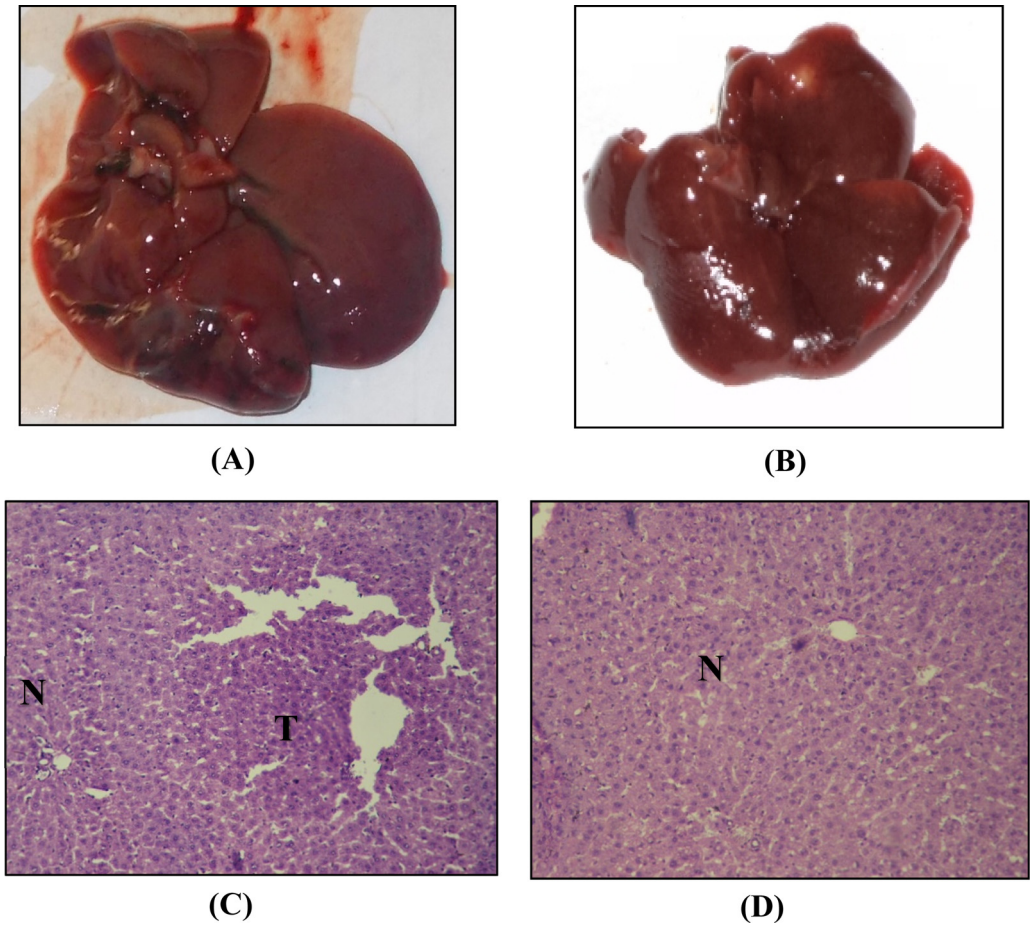

Fig. 13. A&B morphological views of SSSC-33 LD treated liver (Group III), and SSSC-33 HD treated liver (Group IV) respectively; C&D Hematoxylin and Eosin stained liver tissue of SSSC-33 LD treated, and SSSC-33 HD treated respectively observed under LEICA DME microscope (40×). N- non-tumorous tissue T-tumour tissue adjacent to the tumorous fabric.

Conflict of interest

The authors confirm that this article content has no conflict of interest.

Acknowledgments

The authors are grateful to the University Grants Commission, New Delhi, for providing Basic Scientific Research (BSR) fellowship assistance [7-32/2007(BSR)] for the successful completion of this work and also thankful to the Department of Pharmaceutical Sciences and Technology, Birla Institute of Technology, Mesra, for giving lab facilities. We are also thankful to the STIC, CUSAT, Cochin, India and Dr Reddy's Institute of Life Sciences, Hyderabad, India for providing assistance in spectral determination and characterization of synthesised compounds.

Appendix A. Supplementary data

Supplementary data associated with this article can be found, in the online version, at http://dx.doi.org/10.1016/j.biopha.2017.01.108.

References

[1] F. Heindryckx, I. Colle, H. Van Vlierberghe, Experimental mouse models for hepatocellular carcinoma research, Int. J. Exp. Pathol. 90 (4) (2009) 367–386.
[2] D. Hashim, P. Boffetta, C. La Vecchia, M. Rota, P. Bertuccio, M. Malvezzi, E. Negri, The global decrease in cancer mortality: trends and disparities, Ann. Oncol. 27 (5) (2016) 926–933.
[3] H.B. El-Serag, Hepatocellular carcinoma, New Engl. J. Med. 365 (12) (2011) 1118–1127.
[4] A. Raza, Hepatocellular carcinoma review: current treatment, and evidence-based medicine, World J. Gastroenterol. 20 (15) (2014) 4115.
[5] X.K. Guo, H.P. Sun, S. Shen, Y. Sun, F.L. Xie, L. Tao, Q.L. Guo, C. Jiang, Q.D. You, Synthesis and evaluation of gambogic acid derivatives as antitumor agents. Part III, Chem. Biodivers. 10 (1) (2013) 73–85.
[6] J.E. Klaunig, L.M. Kamendulis, B.A. Hocevar, Oxidative stress and oxidative damage in carcinogenesis, Toxicol. Pathol. 38 (1) (2010) 96–109.
[7] D. Ghosh, S.T. Choudhury, S. Ghosh, A.K. Mandal, S. Sarkar, A. Ghosh, K.D. Saha, N. Das, Nanocapsulated curcumin: oral chemopreventive formulation against diethylnitrosamine induced hepatocellular carcinoma in rat, Chem. Biol. Interact. 195 (3) (2012) 206–214.
[8] C.M. da Silva, D.L. da Silva, L.V. Modolo, R.B. Alves, M.A. de Resende, C.V. Martins, Â. de Fátima, Schiff bases: a short review of their antimicrobial activities, J. Adv. Res. 2 (1) (2011) 1–8.
[9] A. Prakash, D. Adhikari, Application of Schiff bases and their metal complexes—a Review, Int. J. Chem. Tech. Res 3 (4) (2011) 1891–1896.
[10] Z.D. Petrović, J. Đorović, D. Simijonović, V.P. Petrović, Z. Marković, Experimental and theoretical study of antioxidative properties of some salicylaldehyde and vanillic Schiff bases, RSC Adv. 5 (31) (2015) 24094–24100.
[11] S. Chacko, S. Samanta, Novel thiosemicarbazide hybrids with amino acids and peptides against hepatocellular carcinoma: a molecular designing approach towards multikinase inhibitor, Curr. Comput. Aided Drug Des. 11 (3) (2015) 279–290.
[12] A.A. Boligon, M.M. Machado, M.L. Athayde, Technical evaluation of antioxidant activity, Med. Chem. 2014 (2014).
[13] M.S. Blois, Antioxidant determinations by the use of a stable free radical, Nature 181 (1958) 1199–1200.
[14] E. Farber, D. Solt, R. Cameron, B. Laishes, K. Ogawa, A. Medline, Newer insights into pathogenesis of liver cancer, Am. J. Pathol. 89 (2) (1977) 477–482.
[15] A.S. Yadav, D. Bhatnagar, Chemo-preventive effect of Star anise in N-nitrosodiethylamine initiated and phenobarbital promoted hepato-carcinogenesis, Chem. Biol. Interact. 169 (3) (2007) 207–214.

[16] A.W. Pound, T.A. Lawson, Partial hepatectomy and toxicity of dimethylnitrosamine and carbon tetrachloride, in relation to the carcinogenic action of dimethylnitrosamine, Br. J. Cancer 32 (5) (1975) 596–603.
[17] S.A. Sheweita, M. Abd El-Gabar, M. Bastawy, Carbon tetrachloride changes the activity of cytochrome P450 system in the liver of male rats: role of antioxidants, Toxicology 169 (2) (2001) 83–92.
[18] W.S. Cheung, R.R. Calvo, B.A. Tounge, S.-P. Zhang, D.R. Stone, M.R. Brandt, T. Hutchinson, C.M. Flores, M.R. Player, Discovery of piperidine carboxamide TRPV1 antagonists, Bioorg. Med. Chem. Lett. 18 (16) (2008) 4569–4572.
[19] M.N. Drwal, P. Banerjee, M. Dunkel, M.R. Wettig, R. Preissner, ProTox: a web server for the in silico prediction of rodent oral toxicity, Nucleic Acids Res. 42 (2014) W53–W58 Web Server issue.
[20] RCSB Proteine Data Bank, 1ZYS: Co-crystal structure of Checkpoint Kinase Chk1 with a pyrrolo-pyridine inhibitor. http://www.rcsb.org/pdb/explore/explore.do?structureId=1zys, 2014 (Accessed March 12, 2014.).
[21] L. Zhang, X. Wang, J. Feng, Y. Jia, F. Xu, W. Xu, Discovery of novel vascular endothelial growth factor receptor 2 inhibitors: a virtual screening approach, Chem. Biol. Drug. Des. 80 (6) (2012) 893–901.
[22] RCSB protien data bank, 2QU5: Crystal structure of the VEGFR2 kinase domain in complex with a benzimidazole inhibitor. http://www.rcsb.org/pdb/explore/explore.do?structureId=2QU5).
[23] M.H. Potashman, J. Bready, A. Coxon, T.M. DeMelfi Jr., L. DiPietro, N. Doerr, D. Elbaum, J. Estrada, P. Gallant, J. Germain, Y. Gu, J.C. Harmange, S.A. Kaufman, R. Kendall, J.L. Kim, G.N. Kumar, A.M. Long, S. Neervannan, V.F. Patel, A. Polverino, P. Rose, S. Plas, D. Whittington, R. Zanon, H. Zhao, Design, synthesis, and evaluation of orally active benzimidazoles and benzoxazoles as vascular endothelial growth factor-2 receptor tyrosine kinase inhibitors, J. Med. Chem. 50 (18) (2007) 4351–4373.
[24] V. Patil, S. Gupta, S. Samanta, N. Masand, Virtual screening of imidazole analogs as potential hepatitis C virus NS5 B polymerase inhibitors, Chem. Pap. 67 (2) (2013) 236–244.
[25] S. Ganguly, S. Murugesan, Docking studies of novel tetrahydroquinoline and tetrahydroisoquinoline analogues into the non-nucleoside inhibitor binding site of HIV-1 RT, Rasayan J. Chem. 1 (2) (2008) 251–257.
[26] M.P. Repasky, M. Shelley, R.A. Friesner, Flexible ligand docking with glide, Curr. Protoc. Bioinf. 8.12 (2007) 1–36.
[27] P.K. Kunda, J.V. Rao, K. Mukkanti, M. Induri, G.D. Reddy, Synthesis, anticonvulsant activity and *in silco* studies of Schiff bases of 2-aminothiophenes via guanidine- catalyzed gewald reaction, Trop. J. Pharm. Res. 12 (4) (2013) 566–576.
[28] S. Shukla, R.S. Srivastava, S.K. Shrivastava, A. Sodhi, P. Kumar, Synthesis, characterization, in vitro anticancer activity, and docking of Schiff bases of 4-amino-1,2-naphthoquinone, Med. Chem. Res. 22 (4) (2012) 1604–1617.
[29] X.-J. Huang, Y.-K. Choi, H.-S. Im, O. Yarimaga, E. Yoon, H.-S. Kim, Aspartate aminotransferase (AST/GOT) and alanine aminotransferase (ALT/GPT) detection techniques, Sensors 6 (7) (2006) 756–782.
[30] E.J. King, A.R. Armstrong, A convenient method for determining serum and bile phosphatase activity, Can. Med. Assoc. J. 31 (4) (1934) 376.
[31] J. King, The Transferases-alanine and Aspartate Transaminases: Practical Clinical Enzymology, D. Van Nostrand Co Ltd, London, UK, 1965.
[32] W.-C. Tai, T.-H. Hu, J.-H. Wang, C.-H. Hung, S.-N. Lu, C.-S. Changchien, C.-M. Lee, Clinical implications of alpha-fetoprotein in chronic hepatitis C, J. Formos. Med. Assoc. 108 (3) (2009) 210–218.
[33] M. Rukmini, B. D'souza, V. D'souza, Superoxide dismutase and catalase activities and their correlation with malondialdehyde in schizophrenic patients, Indian J. Clin. Biochem. 19 (2) (2004) 114–118.
[34] A.K. Sinha, Colorimetric assay of catalase, Anal. Biochem. 47 (2) (1972) 389–394.
[35] R. Van Doorn, C.-M. Leijdekkers, P.T. Henderson, Synergistic effects of phorone on the hepatotoxicity of bromobenzene and paracetamol in mice, Toxicology 11 (1978) 225–233.
[36] W. Habig, M. Pabst, W. Jakoby, The first enzymatic step in mercapturic acid formation. Glutathione-S-transferase, J. Biol. Chem. 249 (1974) 7130–7139.
[37] E. Van Handel, Suggested modifications of the micro determination of triglycerides, Clin. Chem. 7 (3) (1961) 249–251.
[38] A. Kumar, P. Sunita, S.P. Pattanayak, Silibinin inhibits the hepatocellular carcinoma in NDEA-induced rodent carcinogenesis model: an evaluation through biochemical and bio-structural parameters, J. Cancer Sci. Ther. 2015 (2015).
[39] A.C. Parekh, D.H. Jung, Cholesterol determination with ferric acetate-uranium acetate and sulfuric acid-ferrous sulfate reagents, Anal. Chem. 42 (12) (1970) 1423–1427.
[40] V. Sujatha, P. Sachdanandam, Effect of semecarpus anacardium linn. nut extract on experimental mammary carcinoma in Sprague-Dawley rats with reference to tumour marker enzymes, Pharm. Pharmacol. Commun. 6 (8) (2000) 375–379.
[41] W.O. Foye, T.L. Lemke, D.A. Williams, Foye's Principles of Medicinal Chemistry, 6th edition, Lippincott Williams & Wilkins, 2008.
[42] H. Wan, What ADME tests should be conducted for preclinical studies? ADMET DMPK 1 (3) (2013) 19–28.
[43] C.A. Lipinski, Lead-and drug-like compounds: the rule-of-five revolution, Drug. Discov. Today Technol. 1 (4) (2004) 337–341.
[44] L. Di, Strategic approaches to optimizing peptide ADME properties, AAPS J. 17 (1) (2015) 134–143.
[45] M. Radi, E. Dreassi, C. Brullo, E. Crespan, C. Tintori, V. Bernardo, M. Valoti, C. Zamperini, H. Daigl, F. Musumeci, F. Carraro, A. Naldini, I. Filippi, G. Maga, S. Schenone, M. Botta, Design, synthesis, biological activity, and ADME properties of pyrazolo[3,4-d]pyrimidines active in hypoxic human leukemia cells: a lead optimization study, J. Med. Chem. 54 (8) (2011) 2610–2626.
[46] M.D. Segall, C. Barber, Addressing toxicity risk when designing and selecting compounds in early drug discovery, Drug Discov. Today 19 (5) (2014) 688–693.
[47] E.H. Cordes, W.P. Jencks, On the mechanism of schiff base formation and hydrolysis, J. Am. Chem. Soc. 84 (5) (1962) 832–837.
[48] D. Huang, B. Ou, R.L. Prior, The chemistry behind antioxidant capacity assays, J. Agric. Food Chem. 53 (6) (2005) 1841–1856.
[49] S.L. Jothy, Z. Zuraini, S. Sasidharan, Phytochemicals screening, DPPH free radical scavenging and xanthine oxidase inhibitiory activities of Cassia fistula seeds extract, J. Med. Plants Res. 5 (10) (2011) 1941–1947.
[50] M. Jahan, G. Vani, C. Shyamaladevi, Anti-carcinogenic effect of Solanum trilobatum in diethylnitrosamine induced and Phenobarbital promoted hepatocarcinogenesis in rats, Asian J. Biochem. 6 (1) (2011) 74–81.
[51] E. Rocchi, Y. Seium, L. Camellini, G. Casalgrandi, A. Borghi, P. D'Alimonte, G. Cioni, Hepatic tocopherol content in primary hepatocellular carcinoma and liver metastases, Hepatology 26 (1) (1997) 67–72.
[52] R. Kowsalya, J. Kaliaperumal, M. Vaishnavi, E. Namasivayam, Anticancer activity of Cynodon dactylon L. root extract against diethyl nitrosamine induced hepatic carcinoma, South Asian J. Cancer 4 (2) (2015) 83.
[53] R. Khan, I. Kazmi, M. Afzal, F.A. Al Abbasi, G. Mushtaq, A. Ahmad, V. Kumar, F. Anwar, Fixed dose combination therapy loperamide and niacin ameliorates diethylnitrosamine-induced liver carcinogenesis in albino Wistar rats, RSC Adv. 5 (83) (2015) 67996–68002.
[54] E. Waidely, A.-R.O. Al-Yuobi, A. Bashammakh, M.S. El-Shahawi, R.M. Leblanc, Serum protein biomarkers relevant to hepatocellular carcinoma and their detection, Analyst 141 (1) (2016) 36–44.
[55] M.E. Cooper, A. Akdeniz, K.J. Hardy, Effects of liver transplantation and resection on lipid parameters: a longitudinal study, Aust. N. Z. J. Surg. 66 (11) (1996) 743–746.